Human Molecular Genetics, 2013, Vol. 22, No. 15 **3023–3037**
doi:10.1093/hmg/ddt159
Advance Access published on April 4, 2013

Genetic regulation of human adipose microRNA expression and its consequences for metabolic traits

Mete Civelek[1], Raffi Hagopian[1], Calvin Pan[1], Nam Che[1], Wen-pin Yang[4], Paul S. Kayne[4], Niyas K. Saleem[6], Henna Cederberg[6], Johanna Kuusisto[6], Peter S. Gargalovic[5], Todd G. Kirchgessner[5], Markku Laakso[6] and Aldons J. Lusis[1,2,3,*]

[1]Department of Medicine, [2]Department of Human Genetics and [3]Department of Microbiology, Immunology and Molecular Genetics, University of California, Los Angeles, CA 90095, USA, [4]Department of Applied Genomics, [5]Department of Cardiovascular Drug Discovery, Bristol-Myers Squibb, Pennington, NJ 08534, USA and [6]Department of Medicine, University of Eastern Finland and Kuopio University Hospital, Kuopio, Finland

Received February 11, 2013; Revised March 12, 2013; Accepted April 2, 2013

The genetics of messenger RNA (mRNA) expression has been extensively studied in humans and other organisms, but little is known about genetic factors contributing to microRNA (miRNA) expression. We examined natural variation of miRNA expression in adipose tissue in a population of 200 men who have been carefully characterized for metabolic syndrome (MetSyn) phenotypes as part of the Metabolic Syndrome in Men (METSIM) study. We genotyped the subjects using high-density single-nucleotide polymorphism microarrays and quantified the mRNA abundance using genome-wide expression arrays and miRNA abundance using next-generation sequencing. We reliably quantified 356 miRNA species that were expressed in human adipose tissue, a limited number of which made up most of the expressed miRNAs. We mapped the miRNA abundance as an expression quantitative trait and determined *cis* regulation of expression for nine of the miRNAs and of the processing of one miRNA (miR-28). The degree of genetic variation of miRNA expression was substantially less than that of mRNAs. For the majority of the miRNAs, genetic regulation of expression was independent of the expression of mRNA from which the miRNA is transcribed. We also showed that for 108 miRNAs, mapped reads displayed widespread variation from the canonical sequence. We found a total of 24 miRNAs to be significantly associated with MetSyn traits. We suggest a regulatory role for miR-204-5p which was predicted to inhibit acetyl coenzyme A carboxylase β, a key fatty acid oxidation enzyme that has been shown to play a role in regulating body fat and insulin resistance in adipose tissue.

INTRODUCTION

MicroRNAs (miRNAs) are small non-coding RNAs that regulate gene expression by binding to their target messenger RNAs (mRNAs) causing translational repression or target degradation (1). They are initially transcribed as primary miRNAs from distinct loci in the genome or are enzymatically cleaved from introns of protein-coding genes. The transcripts are further processed to form a precursor miRNA (pre-miRNA) that is about 70 to 80 nucleotides long and that forms a unique hairpin-loop structure. The pre-miRNA is exported out of the nucleus and is processed by the Dicer enzyme to form the ~22-nucleotide-long mature miRNA that binds to target mRNAs. Both arms of the pre-miRNA stem–loop structure can give rise to mature miRNAs. miRNAs can target several hundred mRNAs and are considered to fine-tune gene expression (2,3). Understanding the regulation of miRNA expression is crucial in identifying their roles in

*To whom correspondence should be addressed at: Department of Human Genetics, Microbiology Immunology and Molecular Genetics, and Medicine, University of California, Los Angeles, A2-237 Center for Health Sciences, Los Angeles, CA 90095-1679, USA. Tel: +1 3108251359; Fax: +1 3107947345; Email: jlusis@mednet.ucla.edu

gene expression. Numerous biochemical studies have identified the miRNA biogenesis pathway in detail (4); however, variations in the miRNA output in this pathway in the human population that leads to variation in miRNA abundance may have significant consequences for downstream targets. Our understanding of the mature miRNA expression due to genetic variation across the human population is limited.

miRNAs play significant roles in maintaining metabolic homeostasis, and their dysregulation can have severe pathological consequences (5). For example, miRNAs have been shown to regulate lipid metabolism. Liver miRNA-33 targets cholesterol efflux transporter *ABCA1* and controls plasma high-density lipoprotein (HDL) levels (6). Targeting of this miRNA with anti-sense oligonucleotides has been shown to be an effective new pharmacological approach to impact serum lipid levels in rodents and primates (7). Several miRNAs have also been implicated in insulin signaling and glucose homeostasis (8). For example, miRNAs-9 (9,10), −29 (11) and −375 (12) regulate insulin secretion by their expression in pancreatic β-cells, whereas other miRNAs regulate responses to insulin in target tissues. Further, miR-223 has been shown to inhibit glucose uptake in skeletal muscle (13), and miR-33a/b has been found to contribute to fatty acid oxidation in hepatocytes (14). These studies suggest an important role for miRNA-mediated regulation of metabolic disorders.

Insulin-sensitive adipose tissues store excess lipids and secrete hormones that act in distant organs to contribute to the control of energy uptake and expenditure. Disruption of these functions results in disease state that promotes the development of cardiovascular disease and type 2 diabetes. Adipose miRNAs play a role in the development of obesity (15). More than 20 miRNAs have been shown to be associated with adipogenesis primarily by using *in vitro* differentiation of 3T3-L1 cells into adipocytes (reviewed in 16,17). For example, the highly abundant adipose miR-143 was shown to be significantly increased in obese mice (18) and to be involved in human adipocyte differentiation (19). Although many miRNAs have been linked to adipogenesis *in vitro* and in animal obesity models, their functions in human adipose tissue in relation to metabolic syndrome (MetSyn) need to be elucidated to understand their causal role better.

Single-nucleotide polymorphisms (SNPs) that are associated with complex diseases and traits act on intermediate phenotypes, such as mRNA and miRNA transcripts, to affect the disease process (20). Therefore, identification of the SNPs associated with miRNA abundance in disease-relevant tissues has the potential to provide an understanding of the role of miRNAs in pathological processes. Accordingly, we studied the genetic regulation of human adipose miRNA expression and its consequences on metabolic traits relevant to MetSyn in participants of the population-based Metabolic Syndrome in Men (METSIM) study (21). Using next generation sequencing technology, we characterized miRNAs expressed in adipose tissue and the extent of their sequence variation. We also determined significant local (*cis*) regulation of miRNA expression and processing as well as the association of several adipose miRNAs with MetSyn traits, including insulin sensitivity, lipid and lipoprotein levels and obesity.

RESULTS

Small RNA sequencing and quantification

We sequenced small RNA libraries prepared from subcutaneous adipose tissue total RNA of 200 donors. These donors were randomly chosen from 10 197 participants of the METSIM Study, which is a population-based study including men, aged from 45 to 70 years, and living in Kuopio and surrounding communities in eastern Finland. Clinical characteristics of the subjects are presented in Supplementary Material, Table S1. We obtained a total of 795.8 million reads, 660.5 million of which were successfully aligned to the genome. We detected between 184 and 540 unique miRNAs among the samples (Supplementary Material, File 1). Supplementary Material, Figure S1 and Supplementary Material contain the details of mapping statistics. The small RNA library preparation procedure is a multi-step protocol and previous reports indicate that multiplexing of the samples can create bias based on the index sequence used for different samples (22). We prepared libraries from a subset of the samples using two different indexes and showed that barcoding did not have a significant effect on the accurate quantification of miRNA expression levels (Supplementary Material, Figs S2 and S3). We also did not detect a batch effect based on sequencing lane, RNA quality and sequencing depth (Supplementary Material, Fig. S4); therefore, we concluded that sequencing and quantification of the expressed miRNAs in human adipose tissue were reliably achieved without bias.

Adipose tissue miRNA expression

We normalized the miRNA expression levels by calculating the percentage of the reads that mapped to a specific miRNA with respect to the total number of reads that mapped to all miRNAs. Essentially, we calculated the percent abundance of each miRNA in every sample. The distribution of average expression across all samples indicated that three miRNAs, 143-3p, -10b-5p and -486-5p, corresponded to 40% of the reads (Fig. 1 and Supplementary Material, File 1). A total of 350 miRNAs had abundances $<1\%$ of the total reads. Thirty-nine of the 50 most abundant miRNAs in our study were among the 50 most abundant miRNAs in a previous study that sequenced female human adipose small RNAs (23). Twenty-nine miRNAs had read abundance $>0.5\%$ of the total miRNA pool, and several of these miRNAs had previously been shown to play a role in adipose physiology or pathology. For example, miR-143-3p, the most abundant miRNA, has been shown to regulate adipocyte differentiation (19); miR-486-5p, the third most abundant miRNA, has been shown to target *SIRT1*, a regulator of metabolic diseases in obesity (24), in adipose-derived mesenchymal stem cells (25). Several members of the miR-30 family, miRs-30a, -30c, -30d and -30e, were highly expressed in adipose tissue. miRs-30a,-30b,-30c and -30e have been demonstrated to be highly regulated *in vitro* during adipogenesis of adipose-derived stem cells. These results suggested that we were able to quantify the expression of adipose-specific miRNAs.

Genetic regulation of miRNA expression

In order to investigate the genetic loci affecting miRNA expression, we performed expression quantitative trait locus

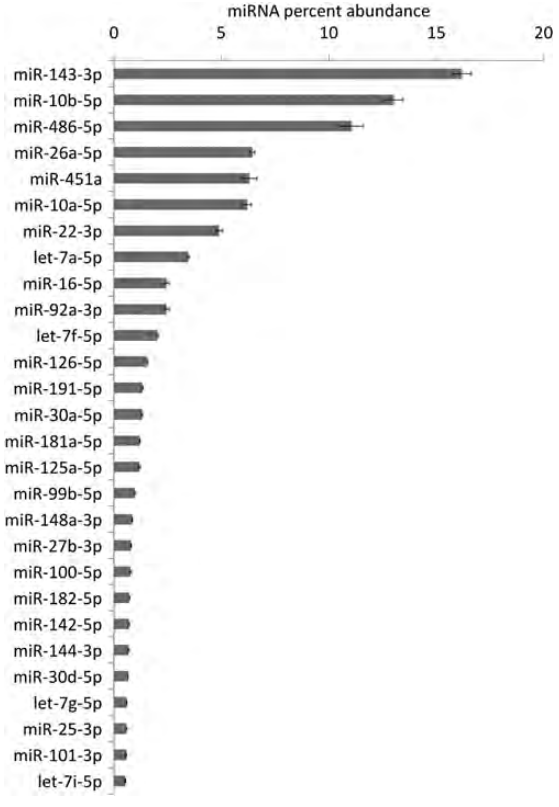

Figure 1. Highly expressed adipose miRNAs. miRNAs with average percent abundance >0.5% are shown. Reads for all the miRNAs in all the samples are given in Supplementary Material, File 1. Bars indicate average ± SEM.

(eQTL) mapping at 640 492 SNP markers for 356 miRNA species. We identified locally acting SNPs (*cis* eQTL) by testing for association within 1 Mb interval on either side of the genomic location of the mature miRNA, using an additive linear model implemented in PLINK (26). Distant acting SNPs (*trans* eQTL) were identified by considering the associations outside of the 2 Mb window. Approximately 164 000 and 289 million SNP-miRNA association *P*-values were calculated for *cis* and *trans* regulation, respectively. *P*-value distribution for *cis* associations was enriched for low *P*-values, whereas the distribution for *trans* associations showed very few significant *P*-values over what would be expected by chance. The enrichment for *cis P*-values suggested the presence of significant *cis* associations among the results (Supplementary Material, Fig. S5). We used all *cis P*-values to estimate the *P*-value cut-off point at 5% false discovery rate (FDR *q*-value) to be 2.04×10^{-5} for *cis* associations. For *trans* associations, we used the Bonferroni-corrected *P*-value of 2.20×10^{-10} since *trans* associations are more prone to noise. We identified nine miRNAs that have significant *cis* eQTLs (Table 1, Supplementary Material, Figs S6–S14); no miRNA had significant *trans* eQTL. Consistent with previous eQTL studies for mRNA expression (27,28), our results showed that the statistical significance of an eQTL was dependent on the distance from the miRNA locations. Within the 2 Mb window surrounding the miRNAs, which we defined as the *cis* eQTL loci, the SNPs which were near the mature miRNA locations had higher statistical significance, suggesting a direct role in transcription as these regions could be transcription start sites (Supplementary Material, Fig. S15).

We performed the association analyses for the expression levels of nine miRNAs by conditioning on the peak SNPs and observed that the significant associations were abolished for seven of the miRNAs suggesting a distinct genetic locus regulating those miRNA expression levels. For miR-5683, a secondary significant association signal at SNP rs640055 ($P = 1.86 \times 10^{-10}$) and, for miR196a-3p, a suggestive association signal at SNP rs17105765 ($P = 2.21 \times 10^{-4}$) were observed predicting that the expression levels of these two miRNAs are controlled by multiple local genetic loci.

Two of the *cis* eQTL miRNAs, 181a-5p and 196a-3p, are encoded from two separate precursors in the genome (29). Since the mature miRNA sequences of these miRNAs are the same, it is not possible to differentiate the genomic location from which the miRNA is transcribed using sequencing reads, because our library preparation method targets the mature miRNAs. miR-181a can be transcribed from two locations on chromosomes 1 or 9. The significantly associated SNP with 181a-5p expression is near the chromosome 1 location of the miRNA gene (Supplementary Material, Fig. S6). There was no significant association near the chromosome 9 locus (Supplementary Material, Fig. S16A). Similarly, miR-196a can be transcribed from two genomic locations on chromosomes 12 and 17, and we observed that the significantly associated SNP is near the chromosome 12 location (Supplementary Material, Fig. S16B). Therefore, based on these associations, we predicted that the actively transcribed precursors for miRNAs 181a-5p and 196a-3p are on the chromosome 1 and 12 loci, respectively. These results indicate that eQTL studies can be used to predict the origin of mature miRNAs in the absence of precursor expression data.

Recent results from the ENCODE project showed that only 27% of small RNAs reside within protein-coding genes (30); however, eight of the nine miRNAs with *cis* eQTLs are transcribed from introns of coding genes in our study (Table 1). This suggests that miRNAs residing within genes exhibit greater common variation in expression than those that are transcribed independently. We reasoned that genetic regulation of miRNA expression could be due to the genetic regulation of the host transcript. To test this hypothesis, we calculated the significance of the associations between the most significant *cis* eQTL SNPs (*cis* eSNPs) and seven of the host mRNA transcripts for which we measured expression levels in the same METSIM participants. We observed that two SNPs had a significant association with both the miRNA and the host gene, whereas five of the seven miRNAs had distinct genetic association from their host gene (Table 2). These results predict that the expression of miRNAs can be regulated distinctly from the host gene.

SNP rs10263705 was associated with expression levels of miR-335-3p ($P = 7.05 \times 10^{-6}$) and *MEST* transcript ($P = 1.95 \times 10^{-4}$), the second intron of which encodes the miRNA. The A allele of rs10263705 was associated with higher expression of both *MEST* and miR-335-3p compared with the G allele (Supplementary Material, Fig. S17). The correlation of *MEST* and miR-335-3p expression levels was 0.53 (8.8×10^{-16}). The significant positive correlation indicated that the causal local variant modulated the host gene and

Table 1. miRNA *cis* eQTLs

miRNA ID	Chromosome	miRNA host gene	SNP ID	Distance from miRNA 5′ end	Association *P*-value	Beta value
miR-5683	6	*F13A1*	rs7769202	80	1.27E − 17	1.239
miR-196a-3p	12	*HOXC5*	rs12300425	9499	5.59E − 09	−0.7316
miR-181a-5p	1	*LOC100131234*	rs1040959	67 607	1.07E − 07	0.2436
miR-941	20	*DNAJC5*	rs2427554	1283	1.14E − 06	−0.3301
miR-204-5p	9	*TRPM3*	rs2993024	120 510	1.33E − 07	1.048
miR-1307-5p	10	*USMG5*	rs2271751	21 033	2.57E − 06	−0.4526
miR-335-3p	7	*MEST*	rs10263705	108 370	7.05E − 06	−0.4387
miR-369-5p	14	Intergenic	rs10146962	361 403	7.97E − 06	−0.4459
miR-455-5p	9	*COL27A1*	rs2225330	864 671	1.99E − 05	−0.4967

miRNAs with significant associations to nearby SNPs are shown. *Cis* eQTL significance *P*-value cut-off is 2.04×10^{-5} corresponding to 5% FDR.

Table 2. Host transcript of *cis* eQTL miRNAs

miRNA ID	Chromosome	miRNA host gene	SNP ID	mRNA association *P*-value	Beta value
miR-1307-5p	10	*USMG5*	rs2271751	7.60E − 56	1.613
miR-335-3p	7	*MEST*	rs10263705	1.95E − 04	−0.2712
miR-196a-3p	12	*HOXC9*	rs12300425	0.4911	0.02027
miR-204-5p	9	*TRPM3*	rs2993024	0.4118	0.05248
miR-455-5p	9	*COL27A1*	rs2225330	0.5198	−0.0312
miR-941	20	*DNAJC5*	rs2427554	0.163	−0.04345
miR-5683	6	*F13A1*	rs7769202	0.1709	−0.08958

Association of miRNA host transcripts with the peak miRNA-associated SNP are shown.

miRNA expression concurrently but additional mechanisms of miRNA transcription or degradation regulated the levels of miR-335-3p.

SNP rs2271751 was associated with the expression levels of miR-1307-5p ($P = 2.57 \times 10^{-6}$) and *USMG5* transcript ($P = 7.60 \times 10^{-56}$), the second exon of which encodes the miRNA (Fig. 2). The T allele of the rs2271751 SNP was associated with higher expression of *USMG5*, whereas it was associated with lower expression of miR-1307-5p compared with the C allele. The correlation of *USMG5* and miRNA-1307-5p expression was −0.26 ($P = 2.05 \times 10^{-3}$). The negative correlation suggests that miR-1307-5p can target its host gene and regulate its expression by a negative feedback loop mechanism, which has been observed for several miRNAs. However, the miRWALK database, which predicts miRNA targets using 10 separate algorithms, did not identify a binding site for miR-1307-5p in the 3′ UTR of *USMG5*, suggesting that this mechanism is unlikely (31). *USMG5* has six exons and can encode three transcript isoforms. The Illumina BeadArray probe (ILMN_1773313) that was used to interrogate the expression levels of this gene maps to exon 2 (Fig. 2C). Recent evidence from deep RNA sequencing of two HapMap lymphoblastoid cell lines (LCLs) showed that local genetic variants cause alternative splicing of *USMG5* transcripts (32). Specifically, SNP rs7911488, which is located on exon 2 and is in perfect linkage disequilibrium with the peak SNP rs2271751 ($r^2 = 1$, 1000 Genomes CEU collection), was predicted to introduce a binding site for exonic splicing enhancers (32) and induce alternative splicing of *USMG5*. Since miR-1307 is located on exon 2 of the *USMG5*, our data support a mechanism where the T allele of rs2271751 is associated with skipping of exon 2 that results in the transcription of miR-1307-5p (Fig. 3).

Genetic regulation of miRNA processing

Multiple recent discoveries recognize that biogenesis and processing of miRNAs can differ from the universally accepted canonical pathway that involves Dicer and Drosha enzymes resulting in miRNA-specific regulatory mechanisms (33). For example, an miRNA precursor can give rise to two mature miRNAs from the 3p and 5p arm, one of which usually has higher expression than the other. It has been reported that different species process the same pre-miRNA distinctly resulting in species-specific dominant expression of the 3p or the 5p arm (34). Furthermore, 3p to 5p ratios of several miRNAs have been shown to be significantly different among various healthy tissues (35) and altered in pathological conditions compared with healthy controls (36). Therefore, we tested whether genetic variants affected the ratio of miRNA expression from the 3p and 5p arms. Using the expression levels of 356 miRNAs detected in our samples, we were able to quantify the ratio of miRNA 3p to 5p abundance of 84 miRNA precursors. There was a significant association of the SNP rs13064131 with the ratio of expression from 3p and 5p arms of miR-28 ($P = 6.14 \times 10^{-5}$, FDR < 10%, Supplementary Material, Fig. S18). 3p to 5p ratios for other precursors did not show significant associations. miR-28 is encoded from the *LPP* gene; SNP rs13064131 was not associated with the expression levels of the *LPP* transcript

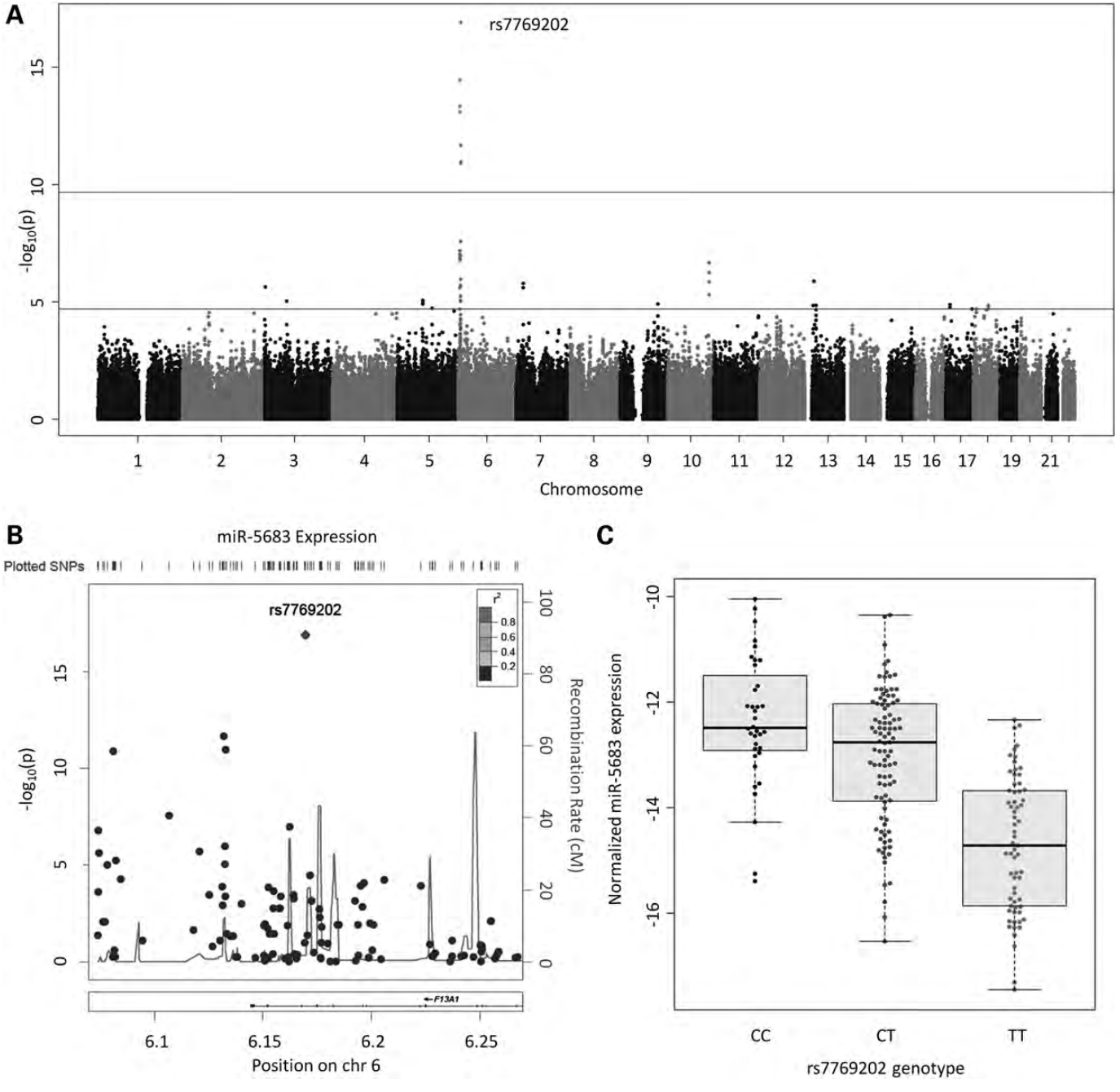

Figure 2. Genome-wide association of miR-5683 expression. (**A**) Manhattan plot showing the significance of association of miR-5683 abundance with SNPs across the genome as indicated by $-\log_{10}(P)$. The lower line denotes *cis* eQTL significance *P*-value of 2.04×10^{-5} and the upper line denotes trans eQTL significance *P*-value of 2.20×10^{-10}. (**B**) Regional association plot focusing on the miR-5683 genomic locus. The plot was generated using LocusZoom (88). Recombination rates are based on European populations from the 1000 Genomes Project. (**C**) Expression level of miR-5683 stratified based on the peak association SNP.

($P = 0.85$). There was also no significant association of rs13064131 with the abundance of miR-28-3p ($P = 0.37$) or miR-28-5p ($P = 0.10$), suggesting that this SNP affects the ratio of 3p to 5p arm expression independent of transcription, possibly via degradation or stabilization mechanisms.

Further diversity in miRNA biogenesis is the length and base composition variation from the reference sequence in miRBase (35,37). miRNAs exhibit heterogeneous lengths where 3′ or 5′ ends are shorter or longer than the reference sequence because of differential trimming by Drosha or Dicer enzymes. Moreover, 3′ ends can be modified as a result of post-transcriptional non-template additions, mostly of uridines or adenosines (33). These non-reference template variations are termed isomiRs (37). We quantified 7 different types of isomiRs and the canonical miRNA reads of the 356 expressed miRNAs (Supplementary Material, Fig. S19). Using the aligned sequencing reads, we counted trimming variants which had 1 base addition or deletion from the 3′ or 5′

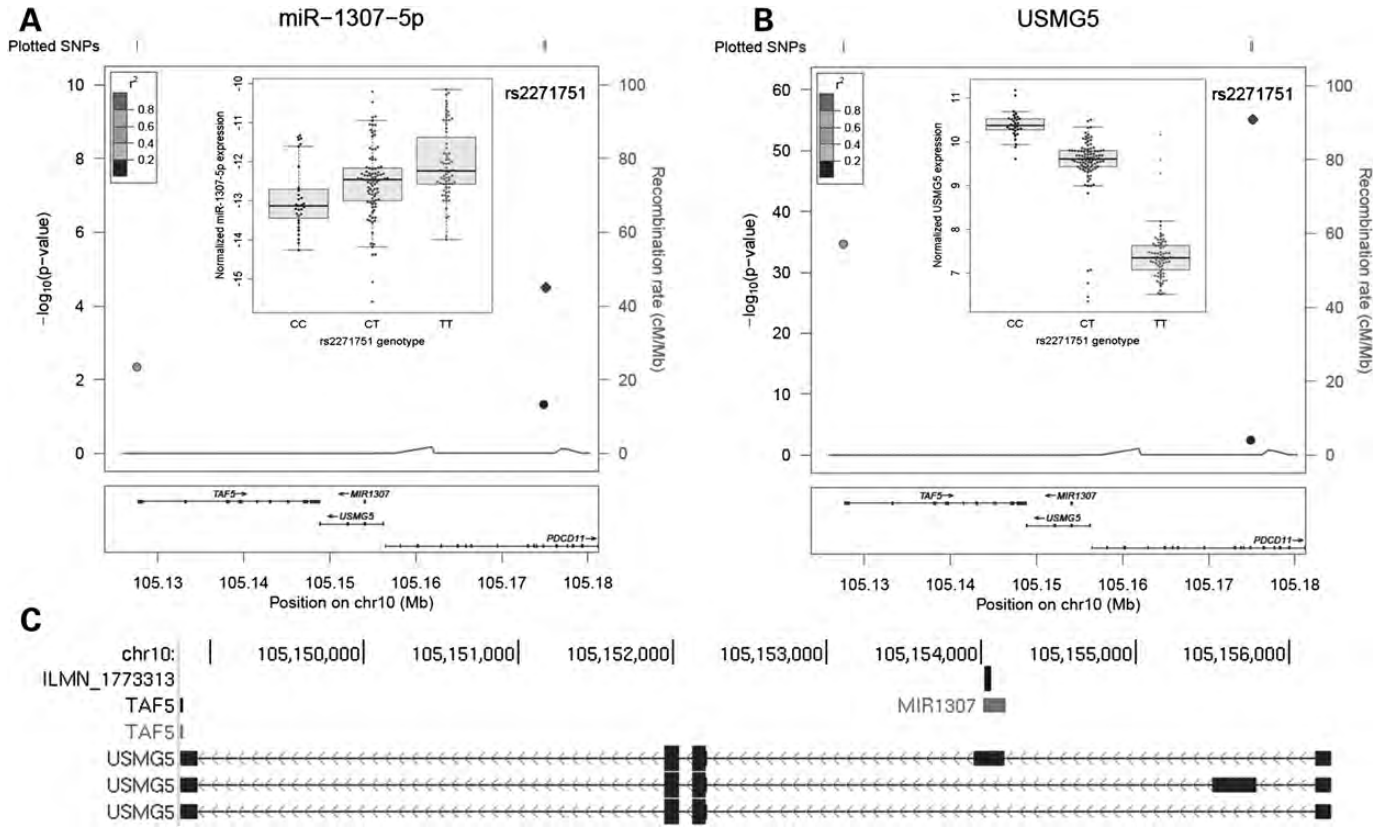

Figure 3. Regional signal plots for USMG5 and miR-1307-5p. Association of the genotyped SNPs and the miRNA expression as indicated by $-\log_{10}(P)$ values are plotted. The plot was generated using LocusZoom (88). Recombination rates are based on European populations from the 1000 Genomes Project. Association of (**A**) miR-1307-5p and (**B**) its host gene, *USMG5*, expression are shown in the *USMG5* locus. (**C**) *USMG5* transcript isoforms in relation to the miR-1307-5p and the microarray probe are shown.

end. We also quantified the non-template addition variants by counting the sequences that aligned to a specific miRNA locus and had an extension at their 3′ end by the addition of any of the four nucleotides (Supplementary Material, File 2).

Widespread variation from the reference miRNA sequence was evident in 108 unique miRNAs (Fig. 4). We detected only miRBase sequence reads in 248 miRNAs. Overall, for the 108 miRNAs, the most common sequence was the canonical sequence represented in miRBase; however, each miRNA had distinct isomiR expression patterns (Fig. 4) displaying large variation among individual samples and miRNA species. For example, 99.8% of the reads that mapped to miR-15b-5p region had the canonical sequence that was represented in miRBase; however, only 5.8% of the reads that mapped to miR-3615 had the canonical sequence, and 70.5% of the reads for miR-3615 had an extra G nucleotide on their 3′ end. The precursor of the miR-3615 has a G nucleotide immediately after the 3′ end of the mature miRNA sequence, suggesting that either the mature miRNA sequence has not been correctly annotated in the miRBase or that this miRNA is processed distinctly in adipose tissue.

The most common isomiRs were 3′ A and U nucleotide additions that made up, on average, 9.0 and 12.3% percent of the total reads that mapped to miRNAs, respectively. C and G additions to the 3′ end were much less with 2.9 and 2.5% of the total reads, respectively (Fig. 4, Supplementary Material, File 2). These results are consistent with previously described isomiR patterns in other mammalian cells and tissues (38) and suggest that the same miRNA species can express multiple different types of isomiRs as a result of differential processing and that the isomiR composition varied across donors. Therefore, to understand whether genetic variants regulated isomiR expression, we calculated the ratio of reads for each type of isomiR to the total number of reads that mapped to a specific miRNA genomic location (Supplementary Material, Fig. S19) and used this quantitative measure to calculate the association of SNP variants. We did not observe any significant SNP associations to isomiR ratio, suggesting that either our study sample was under-powered to detect significant associations or editing events are not under genetic regulation.

Association of miRNA expression with MetSyn-related phenotypes

METSIM participants have been extensively phenotyped for various MetSyn-related traits, including physical measurements, such as body mass index (BMI) and waist-to-hip ratio (WHR), as well as serum lipid and insulin/glucose measurements during an oral glucose tolerance test. We wanted to understand the consequences of variation in miRNA expression on these traits and therefore, calculated the significance

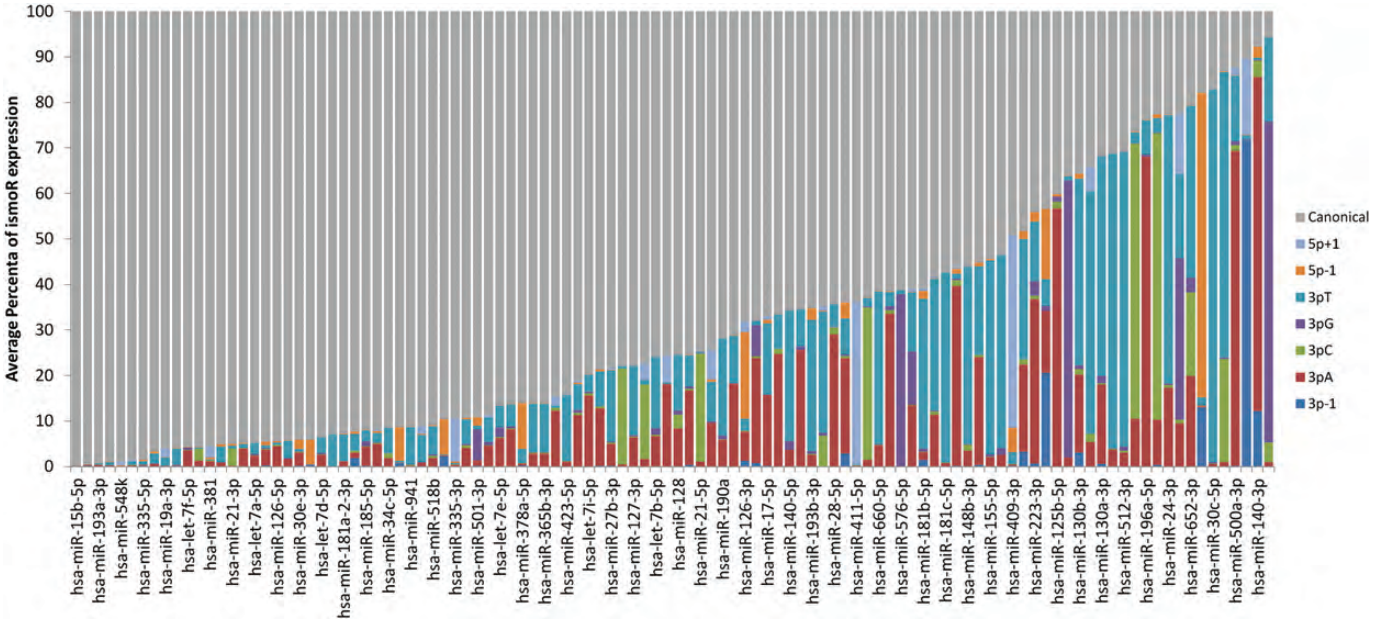

Figure 4. Percentage of isomiR composition for adipose miRNAs. Seven different isomiR modifications were quantified for 356 expressed miRNAs. 108 miRNAs that had isomiRs are shown. Canonical indicates the reads that are the same as in miRBase; 5p+1 indicates reads that had one base extension of the canonical sequence on the 5′ end of the miRNA; 5p−1 indicates reads that had one base deletion of the canonical sequence on the 5′ end of the miRNA; 3pU, 3pG, 3pC, 3pA indicate extension of the canonical sequence with U, G, C, A bases on the 3′ end of the miRNA; 3p−1 indicates reads that had one base deletion of the canonical sequence on the 3′ end of the miRNA. A graphical depiction of the types of quantified isomiR reads is shown in Supplementary Material, Fig. S19.

of associations between the expression levels of miRNAs and 46 measured and derived MetSyn-related phenotypes. For this, we used a generalized linear model adjusting for age as implemented in the *limma* software package (39) and corrected for multiple testing by calculating the FDR using the *qvalue* package (40). We found that 9 and 24 miRNAs were significantly associated with MetSyn phenotypes at 0.1 and 1% FDR, respectively (Supplementary Material, File 3). Eighteen miRNAs which exhibited association with selected subset of the MetSyn-related traits are shown in Table 3. There was considerable overlap among significant miRNAs and associated traits because of the correlation of traits with each other. Of the 18 significantly associated miRNAs, 9, 8 and 8 were associated with Matsuda Insulin Sensitivity Index (41), total triglyceride (TG) levels and BMI, respectively. No significant miRNA association was observed for total and LDL cholesterol levels (Table 3). Our data identified several previously reported associations of various miRNAs with metabolic traits as well as novel associations that will need to be verified with focused hypothesis testing.

Next, we assessed the significance of the correlations between the levels of the *cis* eQTL miRNAs and metabolic traits since significant associations could indicate a mechanism by which the genetic variants influence metabolic traits by regulating miRNA expression. Only miR-204-5p had highly significant associations with BMI, WHR and HDL cholesterol levels (FDR $< 1\%$). (Table 3 and Supplementary Material, Table S2). We looked for association of the peak SNPs for the nine *cis* eQTL miRNAs with BMI (42), WHR (43), lipid and lipoprotein levels (43) and coronary artery disease (CAD) (44) in the published human GWAS. Four *cis* eSNPs had nominal associations ($P < 0.05$) with the metabolic and disease traits but none of the associations reached genome-wide significance. The *cis* eSNP for miR-1307-5p was associated with BMI-adjusted WHR, levels of total cholesterol (TC) and total TG and CAD (Supplementary Material, Table S3). The *cis* eSNP for miR-369-5p was also associated with multiple traits: HDL cholesterol, TC and TG levels as well as CAD. The *cis* eSNP for miR-196a-3p had a nominal association with WHR, but the miRNA levels were not correlated with MetSyn traits. Finally, the *cis* eSNP for miR-204-5p, rs2993024, was associated with HDL cholesterol levels and the association of the expression of this miRNA with HDL cholesterol level was highly significant (Table 3). The A allele of this SNP was associated with raised HDL cholesterol (45) and lower miR-204 expression in our data set (Supplementary Material, Fig. S8). Consistently, miR-204-5p and HDL cholesterol levels were negatively correlated ($r = -0.251$, FDR q-value $= 8.4 \times 10^{-2}$), suggesting a role of this miRNA in the regulation of HDL cholesterol levels.

Correlation of miRNA expression with validated and predicted targets

We sought to understand the mechanism by which *cis* eSNPs affect metabolic traits via their regulation of miRNA expression and thereby their targets. miRNAs function by either degrading their target transcripts (46) or inhibiting translation (47,48); hence a negative correlation exists between miRNA abundance and their target expression. We investigated the population-wide relationship between adipose miRNA abundance and their targets by calculating the correlation of

Table 3. Association of miRNA expression and selected MetSyn traits

miRNA ID	Matsuda index	Total TGs	HDL cholesterol	BMI	WHR	Serum adiponectin	TC	LDL cholesterol
miR-146b-3p	**1.46E − 05**	**2.27E − 04**	**2.27E − 03**	**1.05E − 05**	**1.72E − 05**	**5.21E − 03**	6.76E − 01	2.84E − 01
miR-21-5p	**3.10E − 05**	**2.64E − 03**	7.26E − 02	**2.84E − 04**	**4.46E − 03**	1.18E − 01	6.31E − 01	4.66E − 01
miR-155-5p	**3.95E − 04**	2.49E − 02	1.24E − 02	**1.72E − 05**	**6.83E − 04**	1.19E − 01	6.12E − 01	1.78E − 01
miR-215	**5.82E − 04**	**1.27E − 04**	8.18E − 02	3.18E − 02	3.67E − 02	3.29E − 01	6.80E − 01	7.01E − 01
miR-378a-3p	**1.20E − 03**	**1.21E − 03**	**8.12E − 03**	3.10E − 02	7.82E − 02	1.20E − 01	6.52E − 01	7.31E − 01
miR-378i	**1.20E − 03**	**3.41E − 03**	1.32E − 02	8.27E − 02	1.68E − 01	2.69E − 01	6.85E − 01	7.52E − 01
miR-378d	**5.90E − 03**	**8.11E − 03**	9.25E − 02	2.66E − 01	4.16E − 01	4.13E − 01	6.98E − 01	6.26E − 01
miR-193a-5p	**7.97E − 03**	**9.65E − 04**	**1.63E − 03**	2.39E − 02	1.45E − 01	1.25E − 02	7.21E − 01	7.07E − 01
miR-338-3p	**9.47E − 03**	1.63E − 02	3.02E − 01	1.35E − 01	2.65E − 01	3.48E − 01	5.73E − 01	4.42E − 01
miR-204-5p	1.43E − 02	7.62E − 02	**3.05E − 03**	**2.32E − 07**	**7.38E − 04**	3.55E − 01	6.01E − 01	6.11E − 01
miR-218-5p	2.35E − 02	7.67E − 02	4.25E − 02	**4.74E − 03**	1.19E − 02	1.44E − 01	7.10E − 01	5.03E − 01
miR-421	3.03E − 02	1.56E − 01	4.60E − 01	**8.70E − 03**	1.92E − 01	7.31E − 01	7.30E − 01	5.60E − 01
miR-181c-5p	6.11E − 02	2.78E − 01	5.39E − 01	**9.71E − 03**	**3.41E − 03**	7.03E − 01	7.51E − 01	6.95E − 01
miR-218-1-3p	7.26E − 02	3.14E − 01	**4.53E − 03**	4.01E − 02	8.90E − 02	2.10E − 01	7.36E − 01	1.05E − 01
miR-190a	9.03E − 02	**5.46E − 03**	**1.36E − 04**	1.75E − 01	4.33E − 01	**5.82E − 04**	6.87E − 01	2.24E − 01
miR-153	1.52E − 01	**8.74E − 04**	4.04E − 01	4.74E − 01	7.00E − 01	2.78E − 01	6.31E − 01	7.58E − 01
miR-181c-3p	2.69E − 01	8.70E − 02	2.81E − 01	**3.41E − 03**	**8.72E − 04**	6.85E − 01	5.00E − 01	1.57E − 01
miR-708-5p	3.36E − 01	5.62E − 01	4.46E − 01	**3.70E − 03**	**3.41E − 03**	6.34E − 01	7.23E − 01	6.21E − 01

Values in bold show the significant associations with FDR q-value $< 1\%$.
BMI, body mass index; WHR, waist-to-hip ratio; LDL, low-density lipoprotein; HDL, high-density lipoprotein; TC, total cholesterol; TG, triglyceride.

expression between miRNAs and their validated mRNA targets (49,50) and did not observe a significant negative correlation (Supplementary Material, Figs S20–S23). Next, we examined the relationship between the nine miRNAs (Table 1) and their predicted targets using the miRWalk database, which predicted between 109 and 5062 target genes (Supplementary Material, Table S4). We had mRNA expression information for 79–94% of the predicted targets for each miRNA. We calculated the correlations between the miRNA levels and the predicted target expression, corrected the correlation P-values for multiple testing (40) and focused on the significantly negatively correlated predicted targets (FDR $< 1\%$) since a reciprocal relationship exists for miRNA-mRNA target pairs. There were no negatively correlated targets for miRs-1307-5p and -5683. For the remaining seven miRNAs, we observed between 2 and 276 negatively correlated targets (Supplementary Material, Table S4). We looked for functional enrichment of these genes using Gene Ontology and KEGG Pathway databases and found that miR-196-3p and miR-204-5p targets were significantly enriched for leukocyte activation (GO: 0045321, enrichment FDR $= 0.7\%$) and insulin signaling pathway (KEGG hsa04910, enrichment FDR $= 2.3\%$), respectively. We focused on the miR-204-5p targets since this miRNA had the most significant correlations with BMI, WHR and HDL cholesterol levels (FDR $< 1\%$) and suggestive correlations with the Matsuda index and TG levels (FDR $< 5\%$) (Fig. 5, Supplementary Material, Table S2).

Among the 107 predicted target genes for miR-204-5p, 3 had important functions related to glucose homeostasis. For example, the *PIK3R1* gene encoding the p85 regulatory subunit of phosphatidylinositol 3-kinase (*PI3K*), which couples the insulin and leptin signaling pathways, was one of the predicted targets. *PPARGC1A* (PGC-1α) is a transcriptional co-activator of PPARγ and regulates genes involved in energy metabolism (51). Its expression was negatively correlated with miR-204-5p ($r = -0.35$, P-value $= 4.8 \times 10^{-7}$). Acetyl coenzyme A carboxylase β (*ACACB*) was another predicted target. The gene product is thought to control fatty acid oxidation by catalyzing the carboxylation of acetyl-CoA to malonyl-CoA, the rate-limiting step in fatty acid synthesis. In order to test the hypothesis that mir-204-5p targets *PIK3R1*, *PPARGC1A* and *ACACB*, we over-expressed this miRNA in HeLa cells using three different doses of miR-204-5p mimics and assayed for the changes in transcript abundance by RT–qPCR. Only *ACACB* showed a dose-dependent decrease in transcript levels, whereas the mRNA levels of the other two genes did not change in response to miR-204-5p overexpression (Fig. 5A). Mice deficient in *Acacb* exhibit increased fatty acid oxidation and reduced lipid storage in adipose tissue (52). Furthermore, SNPs in this gene have been associated with BMI and insulin sensitivity in African and European Americans and the adipose expression of this gene was negatively correlated with BMI in the same populations (53). Consistently, we observed that miR-204-5p was positively correlated with BMI ($r = 0.35$, P-value $= 4.8 \times 10^{-7}$), whereas the predicted target, *ACACB*, was negatively correlated ($r = -0.50$, P-value $= 2.6 \times 10^{-14}$), suggesting that SNP rs2993024 regulates miR-204-5p expression, which in turn affects *ACACB* mRNA levels, thereby affecting fatty acid oxidation and metabolic traits (Fig. 5B). Taken together, our results predict a role for miR-204-5p in insulin sensitivity and HDL cholesterol metabolism via its role in targeting *ACACB* transcript in adipose tissue.

DISCUSSION

A single miRNA can target several hundred protein-coding transcripts and therefore can play an important regulatory role in determining how genetic variants affect different phenotypes (54). miRNA regulation of gene expression is considered to be subtle and is thought to play a buffering role in

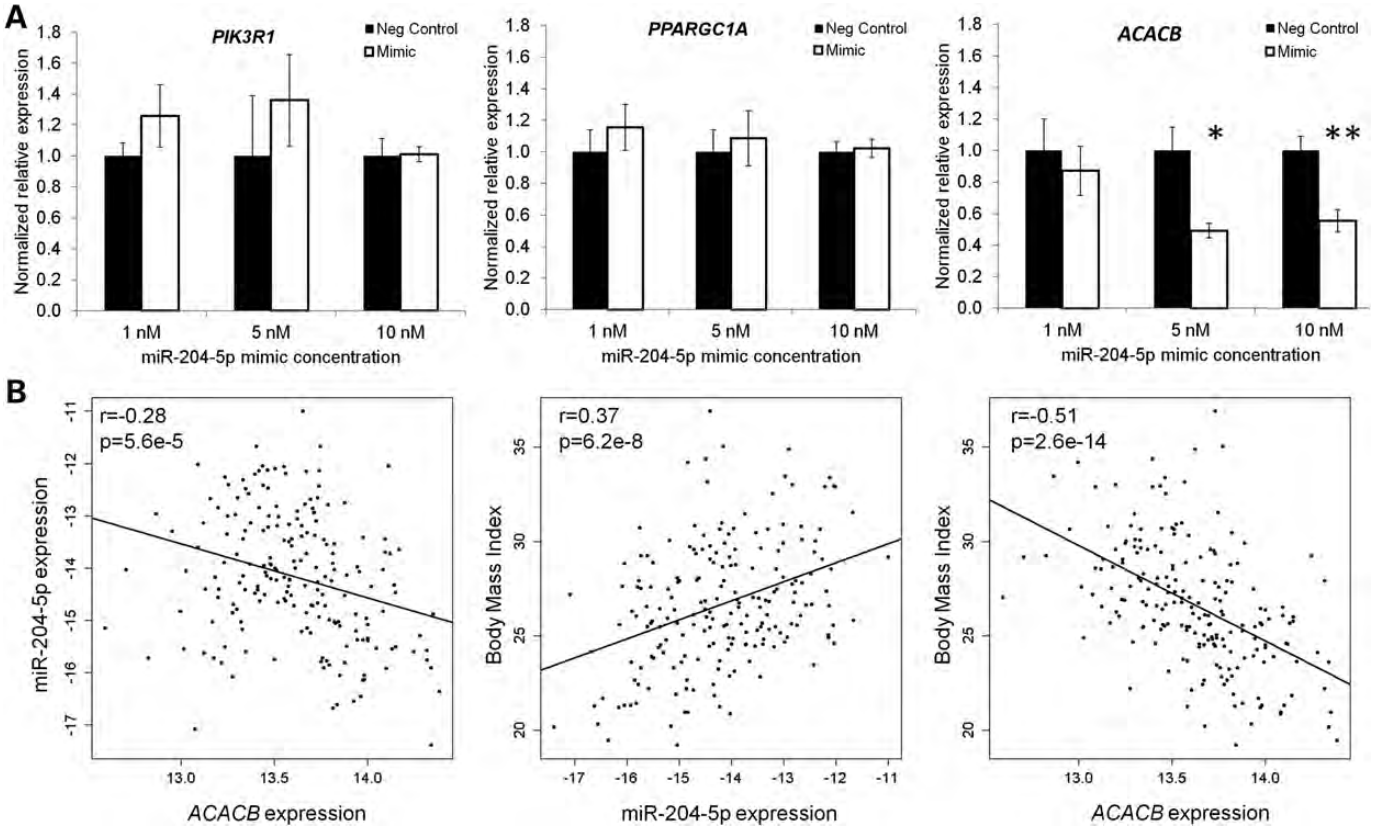

Figure 5. Role of miR-204-5p in regulating metabolic traits. (**A**) HeLa cells were transfected with three different doses of the miR-204-5p mimic, and gene expression was assayed after 24 h. Gene expression was measured by RT–qPCR and normalized to β-2-macroglobulin. Data shown are mean ± SEM. Significance was determined by one-tailed Student's *t*-test. $^{*}P < 0.05$, $^{**}P < 0.01$. (**B**) mir-204-5p and *ACACB* expression in the 199 METSIM participants is plotted against each other and BMI.

response to transcriptional fluctuations (2,3). Understanding the mechanisms that control miRNA expression is important to explain their roles in physiology and disease pathology. In this study, we assembled a large data set to understand the genetic regulation of naturally occurring variation in miRNA expression in the metabolically active adipose tissue obtained from participants of the well-characterized Finnish population-based METSIM study. We determined the genetic regulation of expression for several miRNAs and the association of these miRNAs with mRNA levels and metabolic traits.

miRNA sequencing

Quantification of miRNA abundance using next-generation sequencing presents several challenges. Mapping short-sequence reads to the genome is difficult due to the fact that many reads map to multiple locations. Additionally, miRNA families (such as miR-10 and miR-19) differ by only one nucleotide; therefore, allowing mapping mismatches reduces accuracy of quantifying the miRNA abundance. Inherent mistakes in sequencing technology coupled with polymorphisms in humans also make it difficult to accurately quantify miRNA expression. In order to overcome most, but not all, of these challenges, we used the ambiguity-aware sequence aligner, Novoalign, to map the short reads by allowing no mismatches when a read perfectly maps to a genomic locus and by allowing only one mismatch when there is no perfect alignment. We also weighted the counts in cases where a read maps to multiple genomic locations. This strategy allowed us to overcome the challenge of accurately mapping short reads to the genome while accounting for single-base differences in miRNA families. We were less concerned with accounting for polymorphisms or sequencing errors since studies showed that polymorphisms in genomic loci that overlap the mature miRNA sequences are very rare (23,55) and that sequencing errors are negligible in miRNA sequencing since the mature miRNAs are located in the 5′ end of the cDNA library, where the sequencing errors are significantly less frequent than in the 3′ end (56).

Genetic regulation of miRNA and host transcript expression

The regulation of miRNA expression is much less understood compared with protein-coding transcript expression (4,33). In our study, nine miRNAs corresponding to 2.5% of the miRNAs expressed in adipose tissue showed evidence for local genetic regulation. This was considerably less than 10.5% of the mRNAs which showed *cis* regulation in the same samples, suggesting that expression of miRNA is less dependent on genetic variation. This observation was consistent

with other studies that addressed genetic regulation of miRNA expression (23,57–59). Together, these results suggest that miRNA expression displays small genetic variation, similar to transcription factors due to their central role in affecting multiple aspects of cellular pathways by targeting several mRNAs.

Four previous studies have addressed the genetic architecture of miRNA expression (23,57–59). Borel *et al.* (57) quantified miRNA expression using high-throughput TaqMan qPCR in cultured fibroblasts from umbilical cords of 180 newborns. They found *cis* and *trans* regulation for 12 and 13 of the 121 miRNAs studied, respectively. Gamazon *et al.* (58) quantified miRNA expression using Exiqon miRCURY miRNA microarrays in cultured LCLs from 60 CEU and 60 YRI individuals who are part of the International HapMap project. They found *trans* regulation for 6 of the 201 miRNAs studied but detected no significant *cis* associations. Rantalainen *et al.* (59) quantified miRNA expression using Illumina miRNA BeadArray platform in abdominal and gluteal adipose tissue from 70 men and women. They found *cis* regulation for 3 of the 1146 miRNAs studied but did not detect any *trans* regulation. Finally, Parts *et al.* (23) quantified miRNA expression using Illumina next-generation sequencing in subcutaneous adipose tissue of 131 women. They found evidence for *cis* regulation for 8 of the 418 miRNAs studied. They did not detect any *trans* associations. Our study of 200 men significantly expands these previous findings. We did not find any overlap between our results and the significant miRNA eQTLs reported in fibroblasts and LCLs suggesting tissue specificity of genetic regulation of miRNA expression. This was consistent with previous studies that found tissue independence of *cis* eQTLs for mRNA expression (60). Interestingly, however, only one miRNA, miR-1307, in our study overlapped with the other two adipose tissue miRNA studies. The divergence among various studies was partially the result of defining *cis* and *trans* regulatory regions and *P*-value cut-offs differently. We also reasoned that the differences in adipose tissue studies may be due to unique genetic regulation between females (Parts *et al.* study) and males (our study). It is possible that hormonal effects in adipose miRNA expression overcome genetic effects. Consistent with this hypothesis, effects of gonadal hormones on miRNA expression has been demonstrated (61). Another source of the discrepancy could be technical differences. We used a different miRNA library preparation method than Parts *et al.* (23). Our results demonstrated that different methods of library preparation have a more significant effect on the quantification of miRNA abundance than indexing the same samples with different barcodes and sequencing in distinct batches using the same library preparation method (Supplementary Material, Figs S2 and S3). Various technical difficulties in reliably measuring miRNAs have been previously discussed (56,62); therefore, it is plausible that the different library preparation methods and sequencing platforms contributed to the disagreement between miRNA *cis* eQTLs between the two studies.

Approximately 30% of miRNAs are encoded from genomic regions that contain protein-coding genes (30); however, in our study, we found that eight of the nine miRNAs that had *cis* eQTLs were encoded from protein-coding genes. We found evidence of co-regulation with the host transcript for only two of the eight miRNAs despite previous computational (63) and experimental (64) studies suggesting co-expression of miRNAs and host transcripts. These results suggest differential processing of the primary miRNA transcript from the host transcript or differential utilization of promoter/enhancer sequences for mRNA and miRNA expression. It is probable that genetic variants affect the epigenetic regulation of miRNA expression. Differential methylation of the miRNA loci (65) and histone modifications in the promoter regions of miRNA genes (66) have been described in human cancers due to genetic variation. In order to reliably determine co-regulation and co-expression of miRNAs and host mRNAs, studies that measure primary, precursor and mature miRNA as well as host mRNA levels are needed. Although our study suggests that for the majority of the miRNAs nearby genetic variants affect the regulation of expression of miRNAs and host transcripts in a distinct manner, detailed biochemistry studies are needed to confirm this possibility.

isomiR expression

Similar to protein-coding genes that express multiple isoforms of transcripts, miRNA genes also express different variants called isomiRs. It is believed that these isomiRs arise due to differential processing by Drosha and Dicer, as well as post-transcriptional base additions to 3′ ends of mature miRNAs (4). We quantified seven different types of isomiRs for the miRNAs expressed in our samples by allowing one mismatch in sequence mapping and then restricting the quantification of isomiRs to those that show variability at the 3′ or 5′ end of the sequences. This strategy allowed us to eliminate mappings due to polymorphisms or nucleotide differences among miRNA families which might be in the middle of the reads. Although we observed widespread expression of isomiRs, we did not observe a significant genetic association since we could not reliably quantify isomiRs in all the METSIM subjects because of differences in sequencing depth for each sample. It has been shown that in order to be able to reliably quantify isomiRs, ultra-deep sequencing depth is required (more than 20 million reads per library) (35); the median read depth per library was 2.5 million in our study. miRNA nucleotides 2–8, also termed as the ‘seed sequence’, play a key role in target recognition but the other nucleotides determine the specificity of interaction with the target mRNAs (1). Since the varying lengths of isomiRs have the potential to effect this specificity and thereby affect target repression, it will be important to address whether genetic variants play a role in regulating the isomiR abundance in future studies with deeper miRNA sequencing.

Correlation of miRNA–target transcript pairs

We did not observe evidence of significant negative correlation between abundance of miRNAs and their validated targets even when we restricted our analysis to highly varying miRNAs (Supplementary Material, Fig. S22) or highly expressed targets (Supplementary Material, Fig. S23). This result was consistent with an earlier study that assayed the correlation of adipose miRNA–target mRNA pairs (23). One possibility is that miRNAs can repress gene expression by inhibiting protein translation rather than degrading

mRNAs; however, this possibility is not likely, since we restricted our analysis to those targets for which there was experimental evidence of target repression by direct binding of the miRNA to the 3′ UTR region that resulted in transcript degradation. A more likely explanation is that miRNAs fine-tune target mRNA expression and therefore miRNA regulation of mRNA expression requires the assessment of adipose tissue from more humans to increase the power to detect small effects amid environmental noise.

Relationship to metabolic disorders

Participants of the METSIM study have been extensively characterized for physical and metabolic traits. Our study uncovered known and novel associations between adipose miRNA expression and several of these traits. Among the 24 significantly associated miRNAs, miRs-146b-3p, -215, -21-5p, -193a-5p, -218-5p and -218-3p have been observed to be associated with BMI in a previous human study (23). Additionally, miRs-30a-5p and -378-3p have been shown to regulate adipogenesis and lipid accumulation in adipocytes *in vitro* (67,68). miR-378 is encoded from the first intron of *PPARGC1B*, which encodes the PGC-1β protein, that plays a role in mitochondrial biogenesis (67). Missense mutations in *PPARGC1B* are associated with obesity (69). In addition, Zaragosi *et al.* (67) showed co-expression of miR-378 and *PPARGC1B* in different stages of adipogenesis from mesenchymal stem cells. Together, our data and previous studies support a role for miR-378 in obesity; however, whether this miRNA plays a causal role requires further study.

miRNAs 103 and 107 have been shown to regulate insulin sensitivity via their function in liver and adipose tissue of mice (70); however, we did not observe a significant association with the Matsuda index or glucose and insulin measurements and the expression levels of these miRNAs. Similarly, we did not detect a significant association between BMI and miRs-17-5p, -132 and -143, which have been shown to be down-regulated in adipose tissue of obese patients compared with healthy subjects (71,72). The role of miRs-103 and -107 in regulating insulin sensitivity was established using knock-out and transgenic mouse models. These models represent extreme conditions for the expression of these miRNAs and most likely do not represent the naturally occurring expression variations observed in our study. Similarly, miRNAs associated with obesity have been discovered in other studies using extreme phenotypes and represent a different physiological state than is surveyed in our study.

Among the novel observations, miR-155-5p showed a highly significant association with BMI (FDR q-value $= 4.29 \times 10^{-5}$) and although this miRNA has not been studied in the context of obesity, it has been shown to be involved in other pathological conditions, such as inflammation, infection, cancer and cardiovascular disease (73). We also provide evidence of association for several other miRNAs, such as miRs-215 and -744 with total TGs and insulin levels, respectively, for which little information exists. Although associations observed in our study cannot distinguish between a causal or reactive role for these miRNAs, further studies can provide novel insights into the role of adipose tissue miRNAs and metabolic traits.

We observed the most significant association between the expression level of miR-204-5p and BMI (FDR q-value $= 1.15 \times 10^{-6}$, Supplementary Material, File 3). This miRNA also had a *cis* eQTL, and the peak SNP in the *cis* eQTL locus was nominally associated with HDL levels in a human GWAS (45) (Supplementary Material, Table S3). miR-204-5p has been shown to be down-regulated in the adipose tissue of mice that were fed a high-fat diet (74) and has been shown to directly bind the *PTPN11* transcript (75), which has been implicated in the regulation of body mass, adiposity and leptin signaling (76). It also plays a role in pulmonary hypertension (75), neuroblastoma (77) and vascular calcification (78). *ACACB* was the only gene out of the three predicted genes we tested that was down-regulated by ∼50% in response to miR-204-5p overexpression. The high rate of failure was expected as the prediction of miRNA targets based on computational algorithms has been shown to have high false-positive rates (79,80).

ACACB encodes acetyl-CoA carboxylase β enzyme, which catalyzes the carboxylation of acetyl-CoA to malonyl-CoA and plays a role in mitochondrial fatty acid oxidation in adipose tissue (81). *ACACB* polymorphisms are associated with obesity, diabetes and MetSyn in humans (82,83), and *cis* variants that are associated with increased adipose *ACACB* expression are also associated with higher insulin resistance (53). Additionally, despite some differences in *ACACB* tissue expression patterns between humans and mice (81), *Acacb*-deficient mice have increased adipose fatty acid oxidation and are resistant to diet-induced obesity in agreement with findings in humans (84). Our results showed that *ACACB* was significantly negatively correlated with BMI (Fig. 5) and positively correlated with the Matsuda index (Supplementary Material, File 3). *ACAB* has been proposed to be an effective target in the treatment of MetSyn since lower levels in liver and adipose are associated with improved insulin sensitivity (85). We predict that miR-204-5p, which targets *ACACB*, could serve as a therapeutic agent since the A allele of the SNP rs2993024, which was associated with lower levels of miR-204-5p (Supplementary Material, Fig. S8), has been shown to be associated with higher HDL levels in human GWAS (45).

Our results indicate that natural variation in miRNA expression contributes to MetSyn traits such as obesity and dyslipidemia. Other genetic factors influencing miRNAs and their downstream targets will emerge as additional populations are screened. It is also noteworthy that eQTLs determined in our study show little overlap with previously published studies, most notably adipose miRNA eQTLs from 131 women. It is not possible to conclude whether this is due to moderate sample sizes or sex-specific differences in the regulation of adipose tissue miRNA expression. Moderate sample size undoubtedly led to the identification of only a small subset of the variation in miRNA expression; therefore, larger studies including, both men and women, are needed to explore this further.

MATERIALS AND METHODS

Characteristics of human subjects

We analyzed samples from 200 male human subjects who are part of the METSIM study (21). Ethics Committee of the

Northern Savo Hospital District approved the study. All participants gave written informed consent. The population-based cross-sectional METSIM study included 10 197 men, aged from 45 to 73 years, who were randomly selected from the population register of the Kuopio town in eastern Finland (population 95 000). Every participant had a 1-day outpatient visit to the Clinical Research Unit at the University of Kuopio, including an interview on the history of previous diseases and current drug treatment and an evaluation of glucose tolerance and cardiovascular risk factors. After 12 h of fasting, a 2 h oral 75 g glucose tolerance test was performed and the blood samples were drawn at 0, 30 and 120 min. Plasma glucose was measured by enzymatic hexokinase photometric assay (Konelab Systems reagents; Thermo Fischer Scientific, Vantaa, Finland). Insulin was determined by immunoassay (ADVIA Centaur Insulin IRI no. 02230141; Siemens Medical Solutions Diagnostics, Tarrytown, NY, USA). Height and weight were measured to the nearest 0.5 cm and 0.1 kg, respectively. Waist circumference (at the midpoint between the lateral iliac crest and lowest rib) and hip circumference (at the level of the trochanter major) were measured to the nearest 0.5 cm. Body composition was determined by bioelectrical impedance (RJL Systems) in subjects in the supine position after a 12 h fast. Clinical phenotypes of the subjects used in this study are presented in Supplementary Material, Table S1.

Abdominal subcutaneous adipose tissue was obtained with needle biopsies. Tissue samples were enriched for adipocytes based on the expression of transcripts that are specific for different cell types in the adipose tissue: *CEBPA* and *PPARG* for adipocytes, CDH5 (VE-Cadherin) and *PECAM1* for endothelial cells, *ACTA2* (α-actin) and *CNN1* (Calponin) for smooth muscle cells and *CD68* and *PTPRC* (CD45) for monocyte/macrophages (Supplementary Material, Fig. S24).

miRNA library preparation and sequencing

Total RNA from METSIM subjects was isolated from adipose tissue using the Qiagen miRNeasy kit, according to the manufacturer's instructions. RNA integrity number (RIN) values were assessed with the Agilent Bioanalyzer 2100 instrument. Samples with RIN values >7.0 were used for transcriptional profiling.

Small RNA libraries were prepared from the adipose total RNA of 200 METSIM participants using either the Illumina Small RNA v1.5 protocol or TruSeq Small RNA protocol utilizing up to 48 unique index sequences. Briefly, 3′ and 5′ adapters were added to small RNAs in 500 ng total RNA from each sample, using T4 RNA ligase and truncated T4 RNA ligase 2 (New England Biolabs), respectively. Adapter-ligated small RNAs were reverse-transcribed using Superscript II reverse transcriptase (Invitrogen) and amplified for 12 cycles using HiFi HotStart DNA Polymerase (KAPA Biosystems) using up to 48 unique primers to index samples. Two microliters of PCR product was pooled to be sequenced from either 24 or 48 individuals. Sixteen libraries were prepared in duplicate from the same subjects, using different indexes on different dates. Libraries prepared with the v1.5 method were sequenced for 76-base reads on the Illumina GAIIx platform. Indexed libraries were sequenced for 50-base reads on the Illumina HiSeq2000 platform. Pooled libraries containing 24 samples were sequenced in a single lane. Pooled libraries containing 48 samples were sequenced in two separate lanes and the sequencing reads were combined for subsequent analysis.

Sequence data analysis and miRNA quantification

Sequencing files were converted to the FASTQ format using a custom Perl script. In order to assign the indexed reads to each METSIM subject, a Python script was used to partition the FASTQ file for each lane into multiple FASTQ files, each of which corresponded to one individual. To be included in the partitioned file, a read had to have an exact match to one of the 48 possible index sequences, unambiguously identifying the individual from whom the read originated. Reads which did not exactly match an index sequence were discarded. The reads were then aligned to the hg19 version of the genome using the Novoalign tool with the following settings: -l16 -t30 -h90 -rA -R 1 -m -g 200 -k. These settings allowed for a single read to map to multiple regions of the genome with up to one mismatch. We used the Bioconductor package *GenomicRanges* for R (v.2.14.0) to count the number of reads with alignment coordinates that overlap the coordinates of known mature miRNAs. Whenever a read mapped to 'x' genomic loci, the read would contribute a count of $1/x$ to those regions. The genomic coordinates for known mature miRNAs were downloaded from miRBase version 18 (29). To enable comparison of counts between samples, we normalized the expression values by dividing the counts for a given mature miRNA by the sum of all the miRNA counts for the corresponding individual. For a subsequent analysis, we considered the expression levels of 356 miRNAs that had at least five reads in half of the study participants. We log-transformed the data for the association analysis.

To quantify reads with modifications from the canonical mature miRNA sequences in the miRBase, we looked for exact matches of variant sequences to reads listed in the SAM alignment files. A Python script was used to generate the sequences of several common types of variations, including a single untemplated nucleotide addition to the 3′ end of an miRNA and a one base gain or loss from either the 3′ or 5′ end due to variable Dicer cutting (Supplemetary Material, Fig. S20). Reads which exactly matched the normal mature miRNA or these possible variants were counted for each individual. We then calculated the percentage of modification by dividing the number of modified reads to the total number of reads for each miRNA.

Small RNA sequencing data have been deposited to Gene Expression Omnibus (GEO) with the accession number GSE45159.

mRNA expression analysis

High-quality RNA samples from each METSIM subject were hybridized to Illumina Human HT-12 v3 Expression BeadChips (San Diego, CA, USA). The Genome Studio software (2010.v3) was used for extracting probe fluorescence intensities. HT-12 BeadChip contains 48 804 expression and 786 control probes. Using the re-annotation pipeline developed by Barbosa-Morais *et al.* (86), 19 306 probes were removed due to (i) lack of mapping to any genomic or transcriptomic

location, (ii) mapping to multiple genomic or transcriptomic locations, and (iii) the presence of SNPs in the probe sequence that may affect hybridization efficiency. The remaining 29 497 probes were processed using non-parametric background correction followed by quantile normalization with both control and expression probes utilizing the *neqc* function in the *limma* package (R v2.13.0) (87). In total, 16 223 probes, which correspond to 13 240 unique RefSeq transcripts, with detection *P*-values <0.01 in any of the 200 samples, were used for further analysis. Gene expression data have been deposited to GEO with the accession number GSE32512.

Genotyping

Genomic DNA was isolated from blood with the DNeasy extraction kit (Qiagen) and quantified with NanoDrop 2000 (Thermo Fisher Scientific, Waltham, MA, USA). All samples were randomly arrayed into three 96-well microtiter plates at 50 ng/μl. As per the Affymetrix Genome-wide Human SNP Array 6.0 assay protocol, 2×250 ng of gDNA was digested by restriction enzymes *Nsp*I and *Sty*I separately and products were ligated to respective adaptors. PCR was used for amplifying ligation products and checked for size and quality by QIAxcel (Qiagen). Labeled PCR products were hybridized to the Human SNP 6.0 array. Array hybridization, washing and scanning were performed according to the Affymetrix recommendations. Scanned images were subjected to visual inspection. Affymetrix Genotyping Console (version 4.1) was used to assess the quality of the hybridizations and to make the SNP calls using the default implementation of Birdseed version 2. SNPs used in the association analysis were filtered according to the following criteria, using PLINK v1.08 (26): (i) 234 828 SNPs were removed with minor allele frequencies $<5\%$; (ii) 28 874 SNPs were removed that violated Hardy–Weinberg equilibrium (*P*-value $> 10^{-3}$); and (iii) 9872 SNPs that were genotyped in $<95\%$ of the subjects. The remaining 640 492 SNPs were used for association testing in the METSIM study.

Association analysis

Clustering of the METSIM genotypes with 11 HapMap3 populations demonstrated grouping with CEU (Utah residents with northern and western European ancestry from the CEPH collection) and TSI (Toscani in Italia) populations (Supplementary Material, Fig. S25). Pairwise identical-by-descent estimates using PLINK did not indicate any third-degree or closer relatives in the study population (Supplementary Material, Fig. S26). Log-transformed miRNA and mRNA expression levels were considered as quantitative traits, and genome-wide association analysis was performed for each mRNA or miRNA transcript assuming an additive model and using age as a covariate in PLINK. Association results for mRNA and miRNA expression can be queried in a user-friendly web interface at http://systems.genetics.ucla.edu/data/metsim

miRNA overexpression and RT–qPCR

miR-204-5p mimic and negative control mimic were purchased from Dharmacon. HeLa cells were grown to 80% confluency and were transfected with varying concentrations of mimic and negative control using Lipofectamine 2000 (Invitrogen) for 24 h. Total RNA was isolated using Trizol and reverse-transcribed to cDNA using High-Capacity cDNA Reverse Transcription Kit (Applied Biosystems). Gene expression was measured with SYBR Green (KAPA Biosystems) using LightCycler 480 (Roche Applied Science). Expression values were normalized by the housekeeping gene β2 macroglobulin. Statistical significance was calculated by one-sided Student's *t*-test for downregulation of gene expression. The following primers were used: for *ACACB*, forward 5′TCTCCCGCTGAGTTTGTCAC, reverse 5′GATGTACTCTGCGTTGGCCT; for *PIK3R1*, forward 5′TGGAGCGGAGTTGGAGGAA, reverse 5′CACACGAGC TTCACCCCG; for *PPARGC1A*, forward 5′CCTGCTCGGA GCTTCTCAAA, reverse 5′CCCTTGGGGTCATTTGGTGA.

SUPPLEMENTARY MATERIAL

Supplementary Material is available at *HMG* online.

Conflict of Interest statement. W.-p.Y., P.S.K., P.S.G. and T.G.K. are employees and shareholders of Bristol-Myers Squibb Company. Other authors do not report conflicts of interest.

FUNDING

This work was supported by National Institutes of Health (grant HL28481) to A.J.L., Academy of Finland, Diabetes Research Foundation, Cardiovascular Research Foundation and EVO grant from the Kuopio University Hospital (grant 5263) to M.L., American Heart Association postdoctoral fellowship (grant 10POST3660048) and National Institutes of Health Ruth L. Kirschstein National Research Service Award (grant T32HL69766) to M.C.

REFERENCES

1. Bartel, D.P. (2009) MicroRNAs: target recognition and regulatory functions. *Cell*, **136**, 215–233.
2. Baek, D., Villen, J., Shin, C., Camargo, F.D., Gygi, S.P. and Bartel, D.P. (2008) The impact of microRNAs on protein output. *Nature*, **455**, 64–71.
3. Selbach, M., Schwanhausser, B., Thierfelder, N., Fang, Z., Khanin, R. and Rajewsky, N. (2008) Widespread changes in protein synthesis induced by microRNAs. *Nature*, **455**, 58–63.
4. Davis, B.N. and Hata, A. (2009) Regulation of microRNA biogenesis: a miRiad of mechanisms. *Cell. Commun. Signal.*, **7**, 18.
5. Rottiers, V. and Naar, A.M. (2012) MicroRNAs in metabolism and metabolic disorders. *Nat. Rev. Mol. Cell Biol.*, **13**, 239–250.
6. Moore, K.J., Rayner, K.J., Suarez, Y. and Fernandez-Hernando, C. (2011) The role of microRNAs in cholesterol efflux and hepatic lipid metabolism. *Annu. Rev. Nutr.*, **31**, 49–63.
7. Rayner, K.J., Esau, C.C., Hussain, F.N., McDaniel, A.L., Marshall, S.M., van Gils, J.M., Ray, T.D., Sheedy, F.J., Goedeke, L., Liu, X. *et al.* (2011) Inhibition of miR-33a/b in non-human primates raises plasma HDL and lowers VLDL triglycerides. *Nature*, **478**, 404–407.
8. Williams, M.D. and Mitchell, G.M. (2012) MicroRNAs in insulin resistance and obesity. *Exp. Diabetes Res.*, **2012**, 484696.
9. Plaisance, V., Abderrahmani, A., Perret-Menoud, V., Jacquemin, P., Lemaigre, F. and Regazzi, R. (2006) MicroRNA-9 controls the expression of Granuphilin/Slp4 and the secretory response of insulin-producing cells. *J. Biol. Chem.*, **281**, 26932–26942.
10. Ramachandran, D., Roy, U., Garg, S., Ghosh, S., Pathak, S. and Kolthur-Seetharam, U. (2011) Sirt1 and mir-9 expression is regulated

during glucose-stimulated insulin secretion in pancreatic beta-islets. *FEBS J.*, **278**, 1167–1174.
11. Pullen, T.J., da Silva Xavier, G., Kelsey, G. and Rutter, G.A. (2011) miR-29a and miR-29b contribute to pancreatic beta-cell-specific silencing of monocarboxylate transporter 1 (Mct1). *Mol. Cell. Biol.*, **31**, 3182–3194.
12. Poy, M.N., Eliasson, L., Krutzfeldt, J., Kuwajima, S., Ma, X., Macdonald, P.E., Pfeffer, S., Tuschl, T., Rajewsky, N., Rorsman, P. *et al.* (2004) A pancreatic islet-specific microRNA regulates insulin secretion. *Nature*, **432**, 226–230.
13. Lu, H., Buchan, R.J. and Cook, S.A. (2010) MicroRNA-223 regulates Glut4 expression and cardiomyocyte glucose metabolism. *Cardiovasc. Res.*, **86**, 410–420.
14. Davalos, A., Goedeke, L., Smibert, P., Ramirez, C.M., Warrier, N.P., Andreo, U., Cirera-Salinas, D., Rayner, K., Suresh, U., Pastor-Pareja, J.C. *et al.* (2011) miR-33a/b contribute to the regulation of fatty acid metabolism and insulin signaling. *Proc. Natl Acad. Sci. USA*, **108**, 9232–9237.
15. Heneghan, H.M., Miller, N. and Kerin, M.J. (2010) Role of microRNAs in obesity and the metabolic syndrome. *Obes. Rev.*, **11**, 354–361.
16. McGregor, R.A. and Choi, M.S. (2011) microRNAs in the regulation of adipogenesis and obesity. *Curr. Mol. Med.*, **11**, 304–316.
17. Hilton, C., Neville, M.J. and Karpe, F. (2013) MicroRNAs in adipose tissue: their role in adipogenesis and obesity. *Int. J. Obes. (Lond).*, **37**, 325–332.
18. Takanabe, R., Ono, K., Abe, Y., Takaya, T., Horie, T., Wada, H., Kita, T., Satoh, N., Shimatsu, A. and Hasegawa, K. (2008) Up-regulated expression of microRNA-143 in association with obesity in adipose tissue of mice fed high-fat diet. *Biochem. Biophys. Res. Commun.*, **376**, 728–732.
19. Esau, C., Kang, X., Peralta, E., Hanson, E., Marcusson, E.G., Ravichandran, L.V., Sun, Y., Koo, S., Perera, R.J., Jain, R. *et al.* (2004) MicroRNA-143 regulates adipocyte differentiation. *J. Biol. Chem.*, **279**, 52361–52365.
20. Emilsson, V., Thorleifsson, G., Zhang, B., Leonardson, A.S., Zink, F., Zhu, J., Carlson, S., Helgason, A., Walters, G.B., Gunnarsdottir, S. *et al.* (2008) Genetics of gene expression and its effect on disease. *Nature*, **452**, 423–428.
21. Stancakova, A., Javorsky, M., Kuulasmaa, T., Haffner, S.M., Kuusisto, J. and Laakso, M. (2009) Changes in insulin sensitivity and insulin release in relation to glycemia and glucose tolerance in 6,414 Finnish men. *Diabetes*, **58**, 1212–1221.
22. Alon, S., Vigneault, F., Eminaga, S., Christodoulou, D.C., Seidman, J.G., Church, G.M. and Eisenberg, E. (2011) Barcoding bias in high-throughput multiplex sequencing of miRNA. *Genome Res.*, **21**, 1506–1511.
23. Parts, L., Hedman, A.K., Keildson, S., Knights, A.J., Abreu-Goodger, C., van de Bunt, M., Guerra-Assuncao, J.A., Bartonicek, N., van Dongen, S., Magi, R. *et al.* (2012) Extent, causes, and consequences of small RNA expression variation in human adipose tissue. *PLoS Genet.*, **8**, e1002704.
24. Schug, T.T. and Li, X. (2011) Sirtuin 1 in lipid metabolism and obesity. *Ann. Med.*, **43**, 198–211.
25. Kim, Y.J., Hwang, S.H., Lee, S.Y., Shin, K.K., Cho, H.H., Bae, Y.C. and Jung, J.S. (2012) miR-486–5p induces replicative senescence of human adipose tissue-derived mesenchymal stem cells and its expression is controlled by high glucose. *Stem Cells Dev.*, **21**, 1749–1760.
26. Purcell, S., Neale, B., Todd-Brown, K., Thomas, L., Ferreira, M.A., Bender, D., Maller, J., Sklar, P., de Bakker, P.I., Daly, M.J. *et al.* (2007) PLINK: a tool set for whole-genome association and population-based linkage analyses. *Am. J. Hum. Genet.*, **81**, 559–575.
27. Fairfax, B.P., Makino, S., Radhakrishnan, J., Plant, K., Leslie, S., Dilthey, A., Ellis, P., Langford, C., Vannberg, F.O. and Knight, J.C. (2012) Genetics of gene expression in primary immune cells identifies cell type-specific master regulators and roles of HLA alleles. *Nat. Genet.*, **44**, 502–510.
28. Gaffney, D.J., Veyrieras, J.B., Degner, J.F., Pique-Regi, R., Pai, A.A., Crawford, G.E., Stephens, M., Gilad, Y. and Pritchard, J.K. (2012) Dissecting the regulatory architecture of gene expression QTLs. *Genome Biol.*, **13**, R7.
29. Kozomara, A. and Griffiths-Jones, S. (2011) miRBase: integrating microRNA annotation and deep-sequencing data. *Nucleic Acids Res.*, **39**, D152–D157.
30. Djebali, S., Davis, C.A., Merkel, A., Dobin, A., Lassmann, T., Mortazavi, A., Tanzer, A., Lagarde, J., Lin, W., Schlesinger, F. *et al.* (2012) Landscape of transcription in human cells. *Nature*, **489**, 101–108.
31. Dweep, H., Sticht, C., Pandey, P. and Gretz, N. (2011) miRWalk—database: prediction of possible miRNA binding sites by 'walking' the genes of three genomes. *J. Biomed. Inform.*, **44**, 839–847.
32. Lalonde, E., Ha, K.C., Wang, Z., Bemmo, A., Kleinman, C.L., Kwan, T., Pastinen, T. and Majewski, J. (2011) RNA sequencing reveals the role of splicing polymorphisms in regulating human gene expression. *Genome Res.*, **21**, 545–554.
33. Winter, J., Jung, S., Keller, S., Gregory, R.I. and Diederichs, S. (2009) Many roads to maturity: microRNA biogenesis pathways and their regulation. *Nat. Cell Biol.*, **11**, 228–234.
34. Griffiths-Jones, S., Hui, J.H., Marco, A. and Ronshaugen, M. (2011) MicroRNA evolution by arm switching. *EMBO Rep.*, **12**, 172–177.
35. Cloonan, N., Wani, S., Xu, Q., Gu, J., Lea, K., Heater, S., Barbacioru, C., Steptoe, A.L., Martin, H.C., Nourbakhsh, E. *et al.* (2011) MicroRNAs and their isomiRs function cooperatively to target common biological pathways. *Genome Biol.*, **12**, R126.
36. Li, S.C., Liao, Y.L., Ho, M.R., Tsai, K.W., Lai, C.H. and Lin, W.C. (2012) miRNA arm selection and isomiR distribution in gastric cancer. *BMC Genomics*, **13** (Suppl. 1), S13.
37. Morin, R.D., O'Connor, M.D., Griffith, M., Kuchenbauer, F., Delaney, A., Prabhu, A.L., Zhao, Y., McDonald, H., Zeng, T., Hirst, M. *et al.* (2008) Application of massively parallel sequencing to microRNA profiling and discovery in human embryonic stem cells. *Genome Res.*, **18**, 610–621.
38. Chiang, H.R., Schoenfeld, L.W., Ruby, J.G., Auyeung, V.C., Spies, N., Baek, D., Johnston, W.K., Russ, C., Luo, S., Babiarz, J.E. *et al.* (2010) Mammalian microRNAs: experimental evaluation of novel and previously annotated genes. *Genes Dev.*, **24**, 992–1009.
39. Smyth, G.K. (2004) Linear models and empirical Bayes methods for assessing differential expression in microarray experiments. *Stat. Appl. Genet. Mol. Biol.*, **3**, Article 3.
40. Storey, J.D. and Tibshirani, R. (2003) Statistical significance for genomewide studies. *Proc. Natl Acad. Sci. USA*, **100**, 9440–9445.
41. Matsuda, M. and DeFronzo, R.A. (1999) Insulin sensitivity indices obtained from oral glucose tolerance testing: comparison with the euglycemic insulin clamp. *Diabetes Care*, **22**, 1462–1470.
42. Speliotes, E.K., Willer, C.J., Berndt, S.I., Monda, K.L., Thorleifsson, G., Jackson, A.U., Lango Allen, H., Lindgren, C.M., Luan, J., Magi, R. *et al.* (2010) Association analyses of 249,796 individuals reveal 18 new loci associated with body mass index. *Nat. Genet.*, **42**, 937–948.
43. Heid, I.M., Jackson, A.U., Randall, J.C., Winkler, T.W., Qi, L., Steinthorsdottir, V., Thorleifsson, G., Zillikens, M.C., Speliotes, E.K., Magi, R. *et al.* (2010) Meta-analysis identifies 13 new loci associated with waist-hip ratio and reveals sexual dimorphism in the genetic basis of fat distribution. *Nat. Genet.*, **42**, 949–960.
44. Schunkert, H., Konig, I.R., Kathiresan, S., Reilly, M.P., Assimes, T.L., Holm, H., Preuss, M., Stewart, A.F., Barbalic, M., Gieger, C. *et al.* (2011) Large-scale association analysis identifies 13 new susceptibility loci for coronary artery disease. *Nat. Genet.*, **43**, 333–338.
45. Teslovich, T.M., Musunuru, K., Smith, A.V., Edmondson, A.C., Stylianou, I.M., Koseki, M., Pirruccello, J.P., Ripatti, S., Chasman, D.I., Willer, C.J. *et al.* (2010) Biological, clinical and population relevance of 95 loci for blood lipids. *Nature*, **466**, 707–713.
46. Guo, H., Ingolia, N.T., Weissman, J.S. and Bartel, D.P. (2010) Mammalian microRNAs predominantly act to decrease target mRNA levels. *Nature*, **466**, 835–840.
47. Bazzini, A.A., Lee, M.T. and Giraldez, A.J. (2012) Ribosome profiling shows that miR-430 reduces translation before causing mRNA decay in zebrafish. *Science*, **336**, 233–237.
48. Djuranovic, S., Nahvi, A. and Green, R. (2012) miRNA-mediated gene silencing by translational repression followed by mRNA deadenylation and decay. *Science*, **336**, 237–240.
49. Xiao, F., Zuo, Z., Cai, G., Kang, S., Gao, X. and Li, T. (2009) miRecords: an integrated resource for microRNA-target interactions. *Nucleic Acids Res.*, **37**, D105–D110.
50. Vergoulis, T., Vlachos, I.S., Alexiou, P., Georgakilas, G., Maragkakis, M., Reczko, M., Gerangelos, S., Koziris, N., Dalamagas, T. and Hatzigeorgiou, A.G. (2012) TarBase 6.0: capturing the exponential growth of miRNA targets with experimental support. *Nucleic Acids Res.*, **40**, D222–D229.
51. Puigserver, P. and Spiegelman, B.M. (2003) Peroxisome proliferator-activated receptor-gamma coactivator 1 alpha (PGC-1 alpha): transcriptional coactivator and metabolic regulator. *Endocr. Rev.*, **24**, 78–90.

52. Abu-Elheiga, L., Matzuk, M.M., Abo-Hashema, K.A. and Wakil, S.J. (2001) Continuous fatty acid oxidation and reduced fat storage in mice lacking acetyl-CoA carboxylase 2. *Science*, **291**, 2613–2616.
53. Ma, L., Mondal, A.K., Murea, M., Sharma, N.K., Tonjes, A., Langberg, K.A., Das, S.K., Franks, P.W., Kovacs, P., Antinozzi, P.A. *et al.* (2011) The effect of ACACB cis-variants on gene expression and metabolic traits. *PLoS One*, **6**, e23860.
54. Friedman, R.C., Farh, K.K., Burge, C.B. and Bartel, D.P. (2009) Most mammalian mRNAs are conserved targets of microRNAs. *Genome Res.*, **19**, 92–105.
55. Iwai, N. and Naraba, H. (2005) Polymorphisms in human pre-miRNAs. *Biochem. Biophys. Res. Commun.*, **331**, 1439–1444.
56. Linsen, S.E., de Wit, E., Janssens, G., Heater, S., Chapman, L., Parkin, R.K., Fritz, B., Wyman, S.K., de Bruijn, E., Voest, E.E. *et al.* (2009) Limitations and possibilities of small RNA digital gene expression profiling. *Nat. Methods*, **6**, 474–476.
57. Borel, C., Deutsch, S., Letourneau, A., Migliavacca, E., Montgomery, S.B., Dimas, A.S., Vejnar, C.E., Attar, H., Gagnebin, M., Gehrig, C. *et al.* (2011) Identification of cis- and trans-regulatory variation modulating microRNA expression levels in human fibroblasts. *Genome Res.*, **21**, 68–73.
58. Gamazon, E.R., Ziliak, D., Im, H.K., LaCroix, B., Park, D.S., Cox, N.J. and Huang, R.S. (2012) Genetic architecture of microRNA expression: implications for the transcriptome and complex traits. *Am. J. Hum. Genet.*, **90**, 1046–1063.
59. Rantalainen, M., Herrera, B.M., Nicholson, G., Bowden, R., Wills, Q.F., Min, J.L., Neville, M.J., Barrett, A., Allen, M., Rayner, N.W. *et al.* (2011) MicroRNA expression in abdominal and gluteal adipose tissue is associated with mRNA expression levels and partly genetically driven. *PLoS One*, **6**, e27338.
60. Grundberg, E., Small, K.S., Hedman, A.K., Nica, A.C., Buil, A., Keildson, S., Bell, J.T., Yang, T.P., Meduri, E., Barrett, A. *et al.* (2012) Mapping cis- and trans-regulatory effects across multiple tissues in twins. *Nat. Genet.*, **44**, 1084–1089.
61. Morgan, C.P. and Bale, T.L. (2012) Sex differences in microRNA regulation of gene expression: no smoke, just miRs. *Biol. Sex Differ.*, **3**, 22.
62. Baker, M. (2010) MicroRNA profiling: separating signal from noise. *Nat. Methods*, **7**, 687–692.
63. Rodriguez, A., Griffiths-Jones, S., Ashurst, J.L. and Bradley, A. (2004) Identification of mammalian microRNA host genes and transcription units. *Genome Res.*, **14**, 1902–1910.
64. Baskerville, S. and Bartel, D.P. (2005) Microarray profiling of microRNAs reveals frequent coexpression with neighboring miRNAs and host genes. *RNA*, **11**, 241–247.
65. Lujambio, A., Calin, G.A., Villanueva, A., Ropero, S., Sanchez-Cespedes, M., Blanco, D., Montuenga, L.M., Rossi, S., Nicoloso, M.S., Faller, W.J. *et al.* (2008) A microRNA DNA methylation signature for human cancer metastasis. *Proc. Natl Acad. Sci. USA*, **105**, 13556–13561.
66. Scott, G.K., Mattie, M.D., Berger, C.E., Benz, S.C. and Benz, C.C. (2006) Rapid alteration of microRNA levels by histone deacetylase inhibition. *Cancer Res.*, **66**, 1277–1281.
67. Zaragosi, L.E., Wdziekonski, B., Brigand, K.L., Villageois, P., Mari, B., Waldmann, R., Dani, C. and Barbry, P. (2011) Small RNA sequencing reveals miR-642a-3p as a novel adipocyte-specific microRNA and miR-30 as a key regulator of human adipogenesis. *Genome Biol.*, **12**, R64.
68. Gerin, I., Bommer, G.T., McCoin, C.S., Sousa, K.M., Krishnan, V. and MacDougald, O.A. (2010) Roles for miRNA-378/378* in adipocyte gene expression and lipogenesis. *Am. J. Physiol. Endocrinol. Metab.*, **299**, E198–E206.
69. Andersen, G., Wegner, L., Yanagisawa, K., Rose, C.S., Lin, J., Glumer, C., Drivsholm, T., Borch-Johnsen, K., Jorgensen, T., Hansen, T. *et al.* (2005) Evidence of an association between genetic variation of the coactivator PGC-1beta and obesity. *J. Med. Genet.*, **42**, 402–407.
70. Trajkovski, M., Hausser, J., Soutschek, J., Bhat, B., Akin, A., Zavolan, M., Heim, M.H. and Stoffel, M. (2011) MicroRNAs 103 and 107 regulate insulin sensitivity. *Nature*, **474**, 649–653.
71. Heneghan, H.M., Miller, N., McAnena, O.J., O'Brien, T. and Kerin, M.J. (2011) Differential miRNA expression in omental adipose tissue and in the circulation of obese patients identifies novel metabolic biomarkers. *J. Clin. Endocrinol. Metab.*, **96**, E846–E850.
72. Xie, H., Lim, B. and Lodish, H.F. (2009) MicroRNAs induced during adipogenesis that accelerate fat cell development are downregulated in obesity. *Diabetes*, **58**, 1050–1057.
73. Elton, T.S., Selemon, H., Elton, S.M. and Parinandi, N.L. (2012) Regulation of the MIR155 host gene in physiological and pathological processes. *Gene.*, doi:10.1016/j.gene.2012.12.0.
74. Chartoumpekis, D.V., Zaravinos, A., Ziros, P.G., Iskrenova, R.P., Psyrogiannis, A.I., Kyriazopoulou, V.E. and Habeos, I.G. (2012) Differential expression of microRNAs in adipose tissue after long-term high-fat diet-induced obesity in mice. *PLoS One*, **7**, e34872.
75. Courboulin, A., Paulin, R., Giguere, N.J., Saksouk, N., Perreault, T., Meloche, J., Paquet, E.R., Biardel, S., Provencher, S., Cote, J. *et al.* (2011) Role for miR-204 in human pulmonary arterial hypertension. *J. Exp. Med.*, **208**, 535–548.
76. Feng, G.S. (2006) Shp2 as a therapeutic target for leptin resistance and obesity. *Expert. Opin. Ther. Targets*, **10**, 135–142.
77. Ryan, J., Tivnan, A., Fay, J., Bryan, K., Meehan, M., Creevey, L., Lynch, J., Bray, I.M., O'Meara, A., Davidoff, A.M. *et al.* (2012) MicroRNA-204 increases sensitivity of neuroblastoma cells to cisplatin and is associated with a favourable clinical outcome. *Br. J. Cancer*, **107**, 967–976.
78. Cui, R.R., Li, S.J., Liu, L.J., Yi, L., Liang, Q.H., Zhu, X., Liu, G.Y., Liu, Y., Wu, S.S., Liao, X.B. *et al.* (2012) MicroRNA-204 regulates vascular smooth muscle cell calcification *in vitro* and *in vivo*. *Cardiovasc. Res.*, **96**, 320–329.
79. Lewis, B.P., Shih, I.H., Jones-Rhoades, M.W., Bartel, D.P. and Burge, C.B. (2003) Prediction of mammalian microRNA targets. *Cell*, **115**, 787–798.
80. Krek, A., Grun, D., Poy, M.N., Wolf, R., Rosenberg, L., Epstein, E.J., MacMenamin, P., da Piedade, I., Gunsalus, K.C., Stoffel, M. *et al.* (2005) Combinatorial microRNA target predictions. *Nat. Genet.*, **37**, 495–500.
81. Castle, J.C., Hara, Y., Raymond, C.K., Garrett-Engele, P., Ohwaki, K., Kan, Z., Kusunoki, J. and Johnson, J.M. (2009) ACC2 is expressed at high levels in human white adipose and has an isoform with a novel N-terminus [corrected]. *PLoS One*, **4**, e4369.
82. Riancho, J.A., Vazquez, L., Garcia-Perez, M.A., Sainz, J., Olmos, J.M., Hernandez, J.L., Perez-Lopez, J., Amado, J.A., Zarrabeitia, M.T., Cano, A. *et al.* (2011) Association of ACACB polymorphisms with obesity and diabetes. *Mol. Genet. Metab.*, **104**, 670–676.
83. Phillips, C.M., Goumidi, L., Bertrais, S., Field, M.R., Cupples, L.A., Ordovas, J.M., McMonagle, J., Defoort, C., Lovegrove, J.A., Drevon, C.A. *et al.* (2010) ACC2 gene polymorphisms, metabolic syndrome, and gene-nutrient interactions with dietary fat. *J. Lipid Res.*, **51**, 3500–3507.
84. Abu-Elheiga, L., Oh, W., Kordari, P. and Wakil, S.J. (2003) Acetyl-CoA carboxylase 2 mutant mice are protected against obesity and diabetes induced by high-fat/high-carbohydrate diets. *Proc. Natl Acad. Sci. USA*, **100**, 10207–10212.
85. Wakil, S.J. and Abu-Elheiga, L.A. (2009) Fatty acid metabolism: target for metabolic syndrome. *J. Lipid Res.*, **50** (suppl.), S138–S143.
86. Barbosa-Morais, N.L., Dunning, M.J., Samarajiwa, S.A., Darot, J.F., Ritchie, M.E., Lynch, A.G. and Tavare, S. (2010) A re-annotation pipeline for Illumina BeadArrays: improving the interpretation of gene expression data. *Nucleic Acids Res.*, **38**, e17.
87. Ritchie, M.E., Silver, J., Oshlack, A., Holmes, M., Diyagama, D., Holloway, A. and Smyth, G.K. (2007) A comparison of background correction methods for two-colour microarrays. *Bioinformatics*, **23**, 2700–2707.
88. Pruim, R.J., Welch, R.P., Sanna, S., Teslovich, T.M., Chines, P.S., Gliedt, T.P., Boehnke, M., Abecasis, G.R. and Willer, C.J. (2010) LocusZoom: regional visualization of genome-wide association scan results. *Bioinformatics*, **26**, 2336–2337.